Bioelectric Notes
Note 2
June 12, 2008

A Scaling Law for Bioelectric Effects of Nanosecond Pulses

Karl H. Schoenbach[1],*, Carl E. Baum [#], Ravindra P. Joshi*, and Stephen J. Beebe*

**Frank Reidy Research Center for Bioelectrics, Old Dominion University, Norfolk, VA 23510*
[#]Department of Electrical and Computer Engineering, University of New Mexico, Albuquerque, NM 87131

Abstract

Experimental studies of bioelectric effects caused by single intense, ultrashort (nanosecond and even subnanosecond), square wave pulses indicate that the product of electric field amplitude and pulse duration, i.e., the electrical impulse, can be considered a similarity or scaling factor. An explanation for this scaling law is based on the assumption that any bioelectric effect in this parameter range of intense nanosecond pulses is caused by membrane charging. In particular, it is assumed that electrical charge transferred to the plasma membrane (which, for electroporated membranes is related to the current through the membrane) is a measure of the intensity of the bioelectric effect. For multiple pulses, bioelectric effects caused by ultrashort pulses were found to scale with the square root of the pulse number. This square root dependence on the pulse number points to a statistical motion of cells between pulses with respect to the applied electric field, and can be explained using the random walk theorem. It will only hold if the time between pulses is short compared to the recovery time of the cell membrane, and long compared to the time for considerable, thermally induced changes in the cell position, with respect to the electric field direction. The validity of the scaling law is limited to pulse durations larger than the dielectric relaxation time of the cytoplasm (on the order of 500 ps), and durations less than the charging time constant of cell membranes (on the order of 100 ns for eukaryotic cells). For single pulses with durations close to the characteristic charging time, the bioelectric effects are expected to scale with electrical energy density, rather than the electrical impulse.

Key words: membrane effects; nanoporation; intense electric fields; random walk

Acknowledgement

This work is supported by an Air Force Office of Scientific Research Multidisciplinary University Research Initiative (MURI) grant on “subcellular response to narrow-band and wide-band radio frequency radiation,” administered through Old Dominion University, and an Air Force Office of Scientific Research grant to the University of New Mexico.

Introduction

The effect of intense pulsed electric fields on biological cells and tissues has been the topic of research since the late 1950's. Intense means that the electric field is of sufficient magnitude to cause nonlinear changes in cell membranes. The first paper reporting the reversible breakdown of cell membranes when electric fields are applied was published in 1985 [1]. The first report on the increase in permeability of the plasma membrane of a biological cell, an effect subsequently named "electroporation," appeared in 1972 [2]. The electric fields that are required to achieve electroporation depend on the duration of the applied pulse. Typical pulses range from tens of milliseconds with electric field amplitudes of several tens of kV/m to pulses of a few microseconds and several hundred kV/m.

More recently, the pulse duration range has been extended into the nanosecond range. The effects of such short pulses have been shown to reach into the cell interior [3]. This can be understood by considering the electrical properties of a cell. Fig. 1 shows the cross-section of a mammalian cell, in which the only membrane-bound substructure shown is the nucleus. The cytoplasm, which fills much of the cell, contains dissolved proteins, electrolytes and glucose, and is moderately conductive, as are the nucleoplasm and the cytoplasm in other organelles. On the other hand, the membranes that surround the cell and subcellular structures have a high resistivity. We can therefore think of the cell as a conductor surrounded by an ideally insulating envelope, and containing substructures with similar properties.

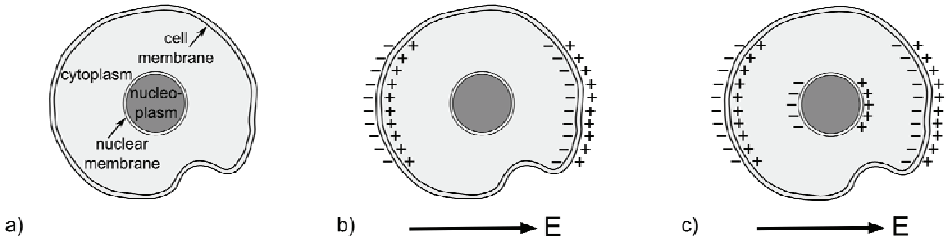

Fig. 1.a) Structure of a biological cell (as would be seen with a light microscope). b) charge distribution as expected for an electric field that rises slowly (compared to cell membrane charging time constant); c) charge distribution as expected for an electric field that rises quickly (compared to cell membrane charging time constant) during the rising part of the applied electric field pulse.

If direct current electric fields or pulses of long duration (compared to the charging time of the capacitor formed by the outer membrane) are applied, eventually, only the outer membrane will be charged; the electric field generated across subcellular membranes during the charging will be zero for an ideal, fully insulating outer membrane. However, during the charging time of the outer membrane, we will also expect potential differences to be generated across subcellular membranes, an effect which will be stronger the shorter the pulse rise time is. Such charging times are in the submicrosecond range for human cells. Of course, for very high electric field pulses that cause electroporation to such an extent that the cell membrane conductivity increases substantially, the electric field will be applied to subcellular structures, not only for the charging time of the outer membrane, but for the entire pulse duration [4].

If the penetrating field is sufficiently large, it can have pronounced effects on intracellular organelles. Nanoseconds to hundreds of nanoseconds long, high electric field pulses (> 1 MV/m) have been shown to permeabilize intracellular organelles [4,5] and release Ca^{2+} from the endoplasmic reticulum (ER) [6,7,8]. They provide a new approach for physically targeting intracellular organelles with many applications, including activation of platelets and release of growth factors for accelerated wound healing [9], and control of apoptosis [10,11,12,13]. More recently, it has been shown that such pulsed electric fields cause shrinkage and even complete elimination of melanoma tumors [14].

Any biological effect of pulsed electric fields on cells depends on the pulse parameters, which, for a square wave pulse, are electric field amplitude, pulse duration, and pulse number. Modeling results using molecular dynamics [15,16,17,18,19] and continuum models [20,21,22,23] have provided insight into the mechanism of permeabilization of membranes with a single pulse. They have led, as will be shown in section 2, to a scaling law for pulse dependent biological effects of single, nanosecond duration pulses. However, in almost any application of nanosecond pulse effects, multiple pulses are required. As will be shown, multiple pulsing cannot be considered as causing a simple additive effect. Consequently, in deciding on the optimum pulse parameters, we are still dependent on educated guesses or time consuming experimental parameter studies.

In the following, and based on the results of experimental studies which cover a diverse range of pulsed field stimulated bioelectric effects, we will suggest an empirical scaling law for pulsed field effects in the nanosecond range. We will then show that it can be derived from some basic principles.

Empirical Scaling Law

To our knowledge, there has been no systematic experimental study on the scaling of nanosecond pulse effects which includes variations of pulse amplitude, pulse duration and pulse number, over an extended range. What exists, are studies where one of the three parameters was kept constant, either pulse number or pulse duration.

For example, a study where the bioelectric effect of 10-ns single pulses was compared to that of 60-ns pulses was published by Beebe et al., in 2004 [24]. In Jurkat cells, it was shown that the uptake of ethidium homodimer, a marker for membrane integrity, and the onset of phosphatidylserine externalization scales with the product of pulse amplitude, E, and pulse duration, τ for single pulse effects. A scaling law for nanosecond single pulse effects, at least for these two bioelectric effects in Jurkat cells, would consequently read:

$$S_1=S_1(E\tau) \qquad (1)$$

with S_1 being a quantity which describes the intensity of the observable bioelectric effect. The product of electrical field amplitude and pulse duration is also known the electrical impact. In the same paper [23], the effect of multiple pulses has been explored, however no attempt was made to determine a scaling law for this case.

A viability study with variable number of pulses, N, but at a fixed pulse duration, has been performed by Pakhomov et al., [25,26]. The viability of human lymphoma cells (U937 and Jurkat cells) after applying 10-ns pulses, has been studied using trypan blue uptake as the indicator for cell death. Trypan blue is normally impermeant to healthy cells. When cell membrane integrity is compromised, the dye is able to enter the cell and bind to protein, making the cell appear blue. Trypan blue was added 24 hours after pulsing to ensure that cell recovery, which occurs on a much faster timescale, is not an issue. Results obtained at various electric field intensities are shown in Figure 2 [26], versus the number of pulses for a single pulse duration, namely, 10 nanoseconds.

The survival curves such as those shown in Figure 2 closely resemble well-known types of dose responses for bioeffects of ionizing radiation [27,28], and can be conveniently described in the same terms.

$$N_{(D)}/N_{(sham)} = 1-(1-\exp(-D/D_0))^n \quad (2)$$

where D is the dose, D_0 is the dose that decreases the survival to 1/e = 37%, and n is the extrapolated intercept of the exponential portion of the curve with the ordinate axis. The indices D_0 and n can be used for quantitative comparison of the sensitivity of different cell lines to nanosecond electrical pulses. Their respective values in our study were 108 J/g and 1.5 for Jurkat cells, and 266 J/g and 1.63 for U937 cells.

These results indicate a scaling law or similarity law of the following form:

$$S_2 = S_2(E^2N) \quad (3)$$

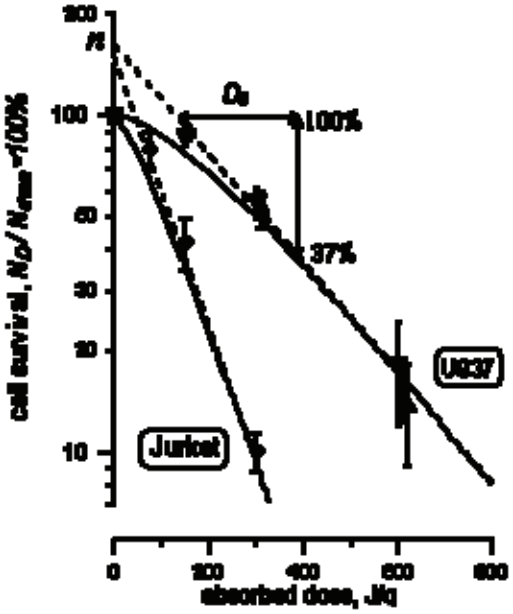

Fig. 2. Survival of Jurkat (left) and U937 cells as a function of the absorbed dose [24]. Different symbols for U937 cells correspond to mean survival values (± s.e.) for different pulsed electric fields (87, 125, and 174 kV/cm). Data points at doses producing average survival under 10% have not been included. The solid lines are the best fits approximations using Eq. (1).

with S_2 being a quantity which describes the intensity of the observable bioelectric effect (in this case, viability of cells or, more accurately, trypan blue uptake), and N being the number of pulses. It means that we should expect similar bioelectric effects if we vary the electric field intensity and the number of pulses, as long we keep the product of the square of the electric field intensity and pulse number the same. We have not included the pulse duration in this similarity law, since the observations on which the law is based, did not include any variation of the pulse duration.

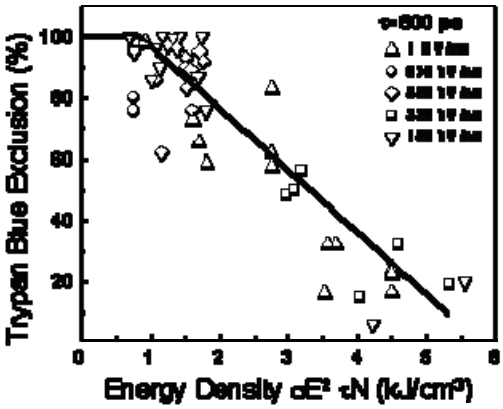

Fig. 3. Trypan blue exclusion in B16 cells versus electrical energy density for pulses of 800-ps duration [27]. Variables were the electric field intensity, which was varied between 150 kV/cm and 1 MV/cm, and the number of pulses, which was varied between 1 and 20,000.

When trypan blue uptake was measured for another type of cell (B16, a murine melanoma cell) using pulses of 800-ps duration, we obtained (as shown in Fig. 3) a similar dependence of trypan blue exclusion on dose (energy density), as with the 10-ns pulses on Jurkat and U937 cells (Fig. 2) [27]. Although the trypan blue exclusion values are plotted versus dose, it needs to be pointed out that the experimental results only provide evidence that the square of the electric field amplitude, E, times the number of pulses, N, can be considered a similarity or scaling of parameter, not necessarily the energy density, $\sigma E^2 \tau N$ (where τ is the pulse duration), which also includes a linear dependence on pulse duration.

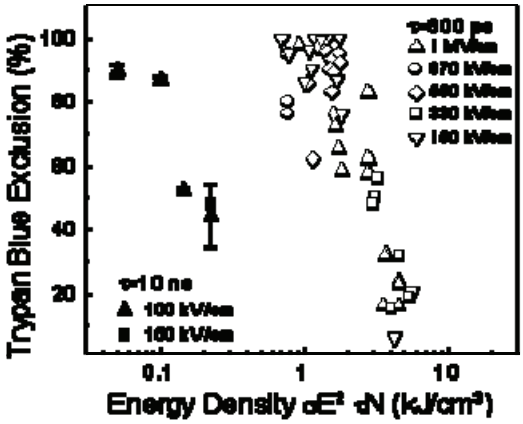

Fig. 4. Trypan blue exclusion versus energy density for B16 cells exposed to 800-ps pulses (same data as plotted in Fig. 3, but on log scale), and exposed to 10-ns pulses [30]. The results show that trypan blue exclusion is not a dose effect.

However, even though the results in Figs. 2 and 3 indicate a dose dependence for ultrashort pulse effects, the results of an experiment performed on B16 cells with pulses of 10-ns duration [29] showed that the observed effects are not dose effects [30]. The 10 ns result falls far off the "dose curve" obtained with 800-ps pulses (Fig. 4).

How is it possible to combine these seemingly contradictory, empirical scaling laws (Eqs. 1 and 2) into a general one for the observed nanosecond bioelectric effects? If both hold (i.e., Eq. 1 for single pulses and variable pulse duration, and Eq. 3 for any number of pulses, but a single pulse duration), a scaling law which would be valid for bioelectric effects caused by pulses of variable amplitude, duration, and number must read:

$S = S(E^2\tau^2N)$

or

$$\mathbf{S = S\,(E\tau N^{1/2})} \qquad (4)$$

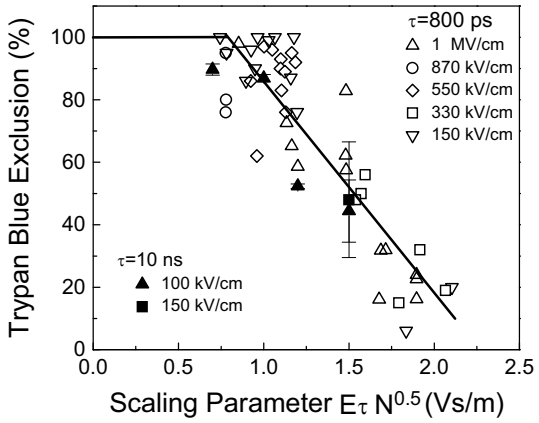

Fig. 5. Trypan blue exclusion for B16 cells versus the scaling parameter $E\tau\sqrt{N}$ [30].

That means that identical effects (uptake of trypan blue) should be expected when the applied electric field, the pulse duration, and the number of pulses is varied in such a way that the product of E, τ, and $N^{1/2}$ stays constant. That this holds is shown in Fig. 5, where the results depicted in Fig. 4 are plotted versus the scaling parameter, $E\tau N^{1/2}$. The 10 ns values, which fall far outside the 800 ps viability data when plotted versus the energy density, or "dose," is now aligned with the results of the 800 ps studies.

As mentioned before, cells that take up trypan blue are usually considered dead or dying. However, in electroporation experiments with propidium iodide as a marker for membrane integrity, uptake of this marker after pulsing has also been reported for viable cells [24]. Since the size of trypan blue molecules (960 Da) is comparable to that of propidium iodide (668 Da), it cannot be assumed that observation of trypan blue uptake is necessarily an indication of cell death, but only of plasma membrane integrity. So it seems reasonable to assume that any direct

effect on the membrane which leads to an increased permeability, such as electroporation, would follow such a scaling law.

Surprisingly, however, the similarity law seems to hold not only for primary processes such as membrane poration, but also for secondary processes, such as the aggregation of platelets when exposed to nanosecond pulses (Fig. 6) [9]. The aggregation was found to be linearly related to the calcium release from subcellular organelles, which in turn was assumed to be due to charging and poration of the organelle membranes. It needs to be pointed out, however, that for a scaling law of this form to be valid, the secondary processes must not be linearly related to the primary (membrane charging) processes. What is required for the application of the scaling law is only that the secondary process is unambiguously caused by the primary effect, which must be a membrane effect.

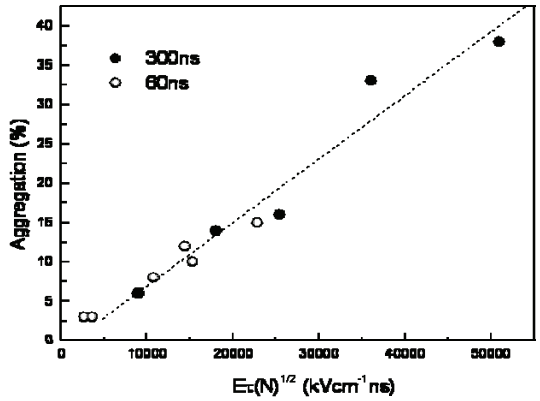

Fig. 6. Aggregation of platelets plotted versus the similarity parameter, $E\tau\sqrt{N}$ (electric field intensity times pulse duration time square root of the number of pulses) for pulses with duration of 60 ns and 300 ns [9].

Discussion

3.1 Single Pulse Operation

What would be a possible explanation for such a scaling law? We will focus first on the single pulse condition (N=1), and then will discuss the pulse number dependence on bioelectric effects.

Let us assume that any observable bioelectric effect (for pulses in our range of observation) has its primary cause in physical and biological changes of membranes (plasma membrane as well as subcellular membranes) and that each effect requires that a certain critical membrane voltage level be reached. For electroporation, the critical membrane voltage is generally assumed to be 1V [31]. However, as shown in experiments [32], pore formation by voltages as low as 0.3 V is also possible. The process simply would take a very long time, as modeled and discussed in a recent publication by the Weaver group [33]. For high electric fields of fast, nanosecond risetime, the membrane may reach a maximum voltage of 1.6 V before poration limits further increase, as shown experimentally by Frey et al., [34]. For other bioelectric effects, such as release of calcium from the ER, the critical trans-membrane voltage might be lower.

When a square wave voltage pulse of duration τ with an electric field, E, is applied across a highly resistive plasma membrane, the voltage at a time, τ, is given as [35]:

$$\Delta V_M(\tau) +/- V_r = fE\,(D/2)\,[1 - \exp(-\tau/\tau_c)]\cos(\theta) \quad (5)$$

where V_r is the resting voltage (which is on the order of 70 mV for many eukaryotic cells), f is the factor which relates to the shape of the cell (it is 1.5 for spherical cells), D is the diameter of the cell, E is the applied electric field, θ is the angle with respect to the direction of the electric field (the amplitude of $\cos(\theta)$ is 1 at the poles of the cell), and τ_c is the charging time constant of the cell [36]:

$$\tau_c = [\{(1+2V)/(1-V)\}\,\rho_1/2 + \rho_2]\,C_m D/2 \quad (6)$$

where V is the volume concentration of the spherical cells, ρ_1 is the resistivity of the suspending medium, ρ_2 the resistivity of the cytoplasm, and C_m is the membrane capacitance per unit area. For a mammalian cell with 10-μm diameter, resistivities of 100 Ωcm, a membrane capacitance of 1μF/cm^2, and a volume concentration small compared to one (typical for an in-vitro experiment), the charging time constant is 75 ns.

Generally, in bioelectric experiments with nanosecond pulses, the applied electric field far exceeds values of 1 MV/m. The calculated voltage across the plasma membrane, from Eq. 5, would then reach values of more than 10 V (assuming a pulse duration, τ, of 100 ns, for a spherical mammalian cell with the parameters listed above), even for "low" electric fields of 1 MV/m. This is an order of magnitude above the critical voltage for membrane poration. It is impossible to achieve, since the membrane conductivity above the critical voltage increases to such a value that voltage clamping occurs. That means that applied electric fields in excess of the critical electric field for electroporation do not cause any further membrane charging, but result in an increase in current density through the membrane.

Instead of using the concept of membrane voltage as a measure of the intensity of a bioelectric effect, we will therefore assume that the intensity of the biological membrane effect can be expressed in terms of the total charge per unit area flowing through the membrane, or, as the integral of the current density over the pulse duration. Since the capacitance of the membrane is only slightly affected by poration, the total charge, Q_m, flowing through the membrane per unit area can be expressed as:

$$Q_m = C_m fE(D/2)[1-\exp(-\tau/\tau_c)]\cos(\theta) - C_m V_c \quad (7)$$

where C_m is the capacitance of the membrane per unit area, and V_c is the critical voltage for poration.

This equation can be rewritten as:

$$Q/Q_{crit} = E/E_0\,[1-\exp(-\tau/\tau_c)]\cos(\theta) \quad (8)$$

with

$$Q/Q_{crit} = (Q_m/ C_m V_c) +1 \quad (9)$$

being the normalized charge (with respect to the critical membrane charge), and:

$$E/E_0 = fE(DV_c/2) \quad (10)$$

being the normalized applied electric field intensity (with respect to the critical electric field intensity). This normalized amplitude of the electric field intensity at the poles ($|\cos(\theta)| = 1$) is plotted in Fig. 7 versus the normalized pulse duration (ratio of pulse duration to characteristic charging time, τ / τ_c) with $Q/Q_0 + 1$ as a variable parameter. The curve for $Q/Q_0+1 = 1$ can be considered a "strength-duration" relationship between the threshold electric field intensity of a square wave pulse and its duration [37]. According to our hypothesis, the curves with $Q/Q_0+1 > 1$ represent curves where identical bioelectric effects can be expected.

Equation 8 is valid only if the impedance of the cytoplasm and the surrounding medium is determined by their resistivities, values which enter the equation for the characteristic charging time (Eq. 6) as ρ_1 and ρ_2, respectively. However, for very short pulse durations, the permittivity of these liquids play an increasingly important role. When the pulse duration is reduced to the dielectric relaxation time, τ_r, of cytoplasm and surrounding medium, respectively, membrane charging effects and dielectric effects become comparable, and for even shorter times, dielectric effects dominate. This means that the voltage across the membranes is not determined by membrane charging anymore, but by the condition that the normal component of the electric displacement is continuous at the cytoplasm-membrane or the membrane-medium interface, or both. The dielectric relaxation time, τ_r, is defined as:

$$\tau_r = \varepsilon/\sigma \quad (11)$$

where ε is the permittivity and σ is the conductivity of the medium or cytoplasm, respectively. For the cells to be considered dielectric bodies, it is necessary that the pulse duration is less than the dielectric relaxation time of the cytoplasm, τ_{rc}.

For pulse durations longer than the dielectric relaxation time of the cytoplasm or the medium, whichever is larger, but shorter than the characteristic charging time (about 0.5 times the charging time, see Fig. 7), which is typically on the order of 100 ns for the plasma membrane of mammalian cells, the exponential function in (8) can be expanded, and the equation can , for $\theta = 0$, be rewritten as:

$$Q/Q_{crit} = (E/E_0)(\tau/\tau_c) \text{ for } \tau_r < \tau < 0.5\tau_c \quad (12).$$

The charge transferred across the membrane, and according to our hypothesis, the intensity of the bioelectric effect, can then be expressed in terms of the product of electric field intensity and pulse duration.

$$S = S(E\tau) \text{ for } \tau_r < \tau < 0.5\tau_c \quad (13)$$

For pulse durations around the characteristic charging time constant the scaling law changes to that of dose effects (see Fig. 7):

$$S = S(E^2\tau) \text{ for } 0.5\tau_c < \tau < 2\tau_c \qquad (14).$$

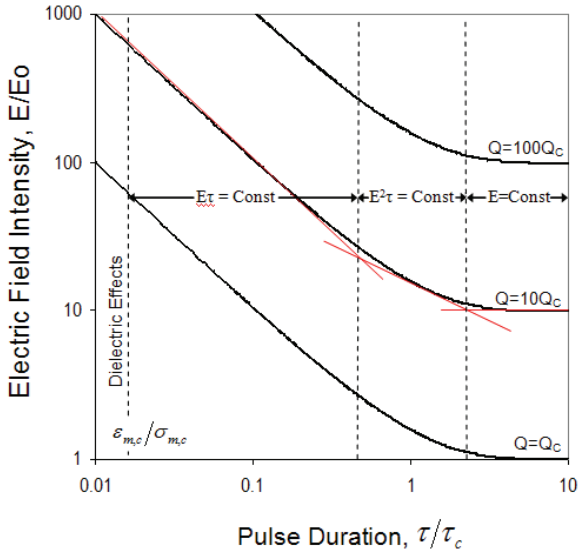

Fig. 7. Electric field intensity - pulse duration range for ultrashort pulse effects. The graph shows curves for constant intensity of bioelectric effects. Parameter is the ratio of total charge to critical charge required to initiate the effect. The validity of these analytic results is limited for short durations to the dielectric relaxation time, ε/σ, of medium or cytoplasm, whichever is larger. For pulse durations less than the characteristic charging time of the cell membrane, τ_c, the curves can be approximated by a scaling law, $S=S(E\tau)$. For the pulse duration range around the characteristic charging time constant the intensity scales approximately with energy density, $S=S(E^2\tau)$ For long pulses, the intensity is dependent only on the electric field intensity, E. However, it needs to be noted, that this relatively simple model, on which the graph is based, does not take into account that the critical voltage for particular bioelectric effects is not a constant. It decreases generally with pulse duration, causing the E/E_0 curves to decline, rather than staying constant as shown in the graph for pulse durations long compared to the characteristic charging time constant.

For even longer times, the intensity of the effects should only be dependent on the amplitude of the electric field. However, since the critical voltage for bioelectric effects also depends on the pulse duration, a fact which is not considered in the simple model, it is expected that the critical electrical field intensity decreases with increasing pulse duration, however slightly.

A similar law also holds for subcellular, membrane-bound structures. In this case, this scaling law can be derived from an analytic expression for the charge accumulated at the poles of a spherical organelle membrane in response to an external electric field, E, of duration, τ [11]:

$$Q_0(t) = C_{mo}f^2Ed\tau_c(\exp(-\tau/\tau_c)–\exp(-\tau/\tau_0))/2(\tau_c - \tau_0) - C_{mo}V_{co} \qquad (15)$$

where d is the diameter of the organelle, f is a geometry constant (for spherical cells and organelles in the center, f = 3/2), and τ_o and τ_c are the charging time constants for organelle

membrane and cell membrane, respectively. These time constants depend on size of the cell and organelle, membrane capacitance, and resistivity of medium and cytoplasm. For times short compared to these charging times, the exponential functions can be expanded, with only the first and second term in the expansion being considered. Also assuming, as we did for the plasma membrane, that the charge required to reach poration of the organelle is small compared to the total charge, we obtain:

$$[Q/Q_{crit}]_{org} = (E/E_o)(\tau/\tau_o) \qquad (16)$$

with $[Q/Q_{crit}]_{org}$ being $(Q_{mo}/C_{mo}V_{co}) + 1$, and E/E_o being $f^2E(dV_c/2)$. Accordingly, for times long compared to the dielectric relaxation time of the cytoplasm and short compared to the charging times of the organelle membranes, the increase in charge on the membranes of organelles can, as for the plasma membrane, be expressed in terms of the product of pulse duration and electric field.

3.2 Multiple Pulse Operation

For multiple pulses, one would expect that there is an additive effect: that each successive shot increases the charges on the membrane by a certain amount, which is dependent on the type of cells and on the time between pulses, or the degree of recovery between pulses, respectively. From this assumption, one would expect a wide range of N-dependences, N being the number of pulses. In the best case, if the pulsed electric field always affects the membrane at the same position, and for a repair time long compared to the time between pulses, the effect would at least scale linearly with N, but could even become nonlinear (increasing with N^x, where $x>1$); in the worst case, where the repair time is very short compared to the time between pulses, there wouldn't be any additive effect. However, all our experimental results indicate that the dependence on N can be described by a square root law only. This does not only hold true for primary effects, such as permeabilization of membranes, but also secondary effects, such as platelet aggregation.

In order to understand, let us consider the local effect of electric fields on cells, particularly cell plasma membranes. Let us assume that each nanosecond pulse causes a localized effect on the plasma membrane, i.e., nanoporation. The effect will be most pronounced at the poles of the cell, since at these points the membrane voltage has a maximum [Eq. 5].

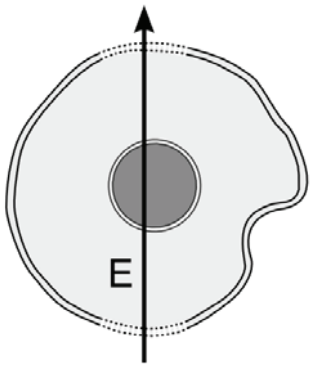

Fig. 8. Schematic sketch of a cell showing effects, such as poration at the poles (defined by direction of applied electric field).

This is schematically shown in Fig. 8, where the stippled area, at one of the poles of the cells, is assumed to be affected. The rest of the cell membrane is unaffected by the pulse. If we increase the intensity of the electric field, more and more of the cell membrane will be affected until, for very large electric fields, the entire plasma membrane will show a response to the pulse. An example is shown in Fig. 9, where the membrane voltage distribution for a cell that was hit by a 50-ns pulse of 100-kV/cm amplitude is shown [34]. The intensity of the voltage dependent dye that was used in these experiments (Annine 6) is evenly distributed over the anode and cathode half-spheres of the cells (Jurkat cells) for the control, indicating that the entire cell membrane is porated and not just the pole areas. In most of the cases that we have studied, however, the electric field is lower and only the poles are affected, as indicated in Fig. 8.

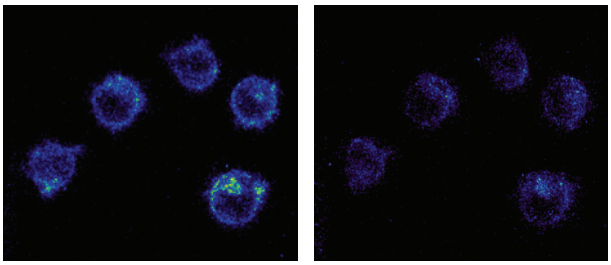

Fig. 9. Jurkat cells before (left) and 25 ns into (right) an electric field application. The images show a drastic decrease of the fluorescence intensity during the pulsed electric field, which indicates high membrane voltages. During the pulse, the intensities are different for anode- and cathode-directed hemispheres, but within the hemispheres, are independent of the azimuthal angle [34]. The direction of the electric field, with an amplitude of E_0, is shown in the insert.

This holds for a single pulse. If multiple pulses of the same amplitude, E_0, are applied, the time between pulses is generally on the order of one second. During this time, the position of the cell with respect to the direction of the electric field vector has most likely changed. The next pulse, therefore, sees a cell that has rotated with respect to the electric field, and consequently the poles of the cell are not identical anymore with those defined by the first pulse (Fig. 10a). Instead of rotating the cell in our frame of reference, which is defined by the direction of the electric field, we can also use the cell itself as frame of reference (Fig. 10b).

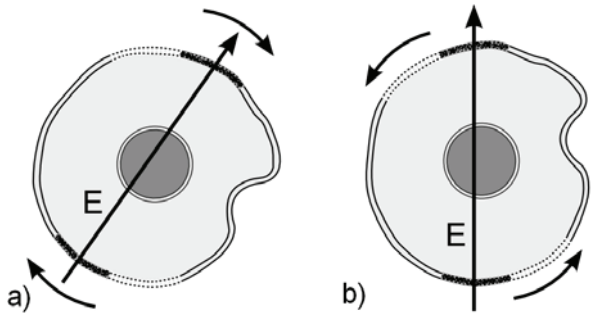

Fig. 10.a) Schematic sketch of a cell, which has rotated with respect to the applied electric field direction. The effect caused by the previous (first) pulse (see Fig. 8) has not yet subsided, and a new effect at the poles of the slightly rotated cell is generated by a second pulse. Fig. 10. b) Same as Fig. 10. a) except cell position is used as reference frame, and the electric field direction which was fixed before varies now randomly.

For multiple pulses (N pulses), keeping the cell as the frame of reference, we can add the randomly distributed electric field vectors (each of them with the same magnitude, E_0) and describe the observed effect of the result of a single electric field vector with an amplitude, E. It is known that the resulting field vector, E, for identical electric field vectors with amplitude E_0, but randomly varying field directions is given as [38]:

$$E = N^{1/2} E_0 \tag{17}$$

This is treated in detail in Appendix A. It is basically the random-walk problem. After summarizing the classical two-dimensional result, several canonical three-dimensional results are derived. All give the $N^{1/2}$ dependence on the number of pulses. In addition, there is a geometric factor, not too different from unity times the $N^{1/2}$. This factor is summarized in Appendix A.5.

Summary

Empirical results of bioelectric studies with single square wave electrical pulses of nanosecond and subnanosecond duration indicate a scaling law of the type:

$$S = S(E\tau) \tag{1}$$

where E is the electrical field intensity, τ is the pulse duration, and S denotes the intensity of some observable effect, such as membrane permeabilization: identical results can be expected for experiments where the product of E and τ is kept constant. This empirical equation can be derived from first principles, with the hypothesis that the intensity of bioelectric effects is determined by the total charge, transported across the membrane per unit area. It is further assumed that this charge is much higher than the critical charge required for the onset of a bioelectric effect, e.g., electroporation.

This scaling law is valid for pulse durations in excess of the dielectric relaxation time of the medium in which the cells are embedded or that of the cytoplasm, whichever is larger, and less than the characteristic charging time constant of cell membranes. For pulse durations around the characteristic charging time constant, the intensity of observable bioelectric events follows a similarity law which resembles that of dose effects. This might explain the dose dependence of the conductivity of the plasma membrane measured with 60-ns and 600-ns single pulses [39].

For multiple exposures to the electric field pulses, the intensity of observable bioelectric effects in a well defined cell suspension (one cell type, no variation in the properties of the surrounding medium) follows the scaling law:

$$S=S(E\tau N^{1/2}) \text{ for } \tau_r < \tau < 0.5\tau_c \tag{18}$$

If we include the characteristic charging time (which includes information on the cell type and medium through the capacitance of the plasma membrane per unit area), C_m, the resistivity of the cytoplasm, ρ_2, and the resistivity of the surrounding medium, ρ_1, as variable parameters:

$$\tau_c = [\{(1+2V)/(1-V)\}\rho_1/2+ \rho_2]\, C_m D/2 \quad (6)$$

the scaling law reads:

$$S=S(EN^{1/2}\tau/\tau_c) \text{ for } \tau_r < \tau < 0.5\tau_c \quad (19)$$

Varying the surrounding medium allows us to modify not only the validity range (i.e., by increasing the resistivity of the surrounding medium, we are able to expand this range by shifting the upper limit to longer times), but also the intensity of the effect for a given cell type: media with larger resistivity will cause a reduction in the intensity, S, of the observable effect with all other parameters kept constant.

The square root of N dependence, where N is the number of pulses, can be explained by assuming that the position of cells with respect to the direction of the applied electric field changes randomly between pulses. As shown in the appendix, this "random walk" law does not only hold for spherically shaped cells, but also for disk-like cells, such as platelets, and rod-shaped cells, such as certain bacteria.

The validity of the "random walk" law requires that the recovery time of the cell membrane is long compared to the time between pulses. It also requires that the motion of the cells between shots (rotation with respect to the electric field direction) is completely random. If there is only minor cell rotation between pulses, the effect of multiple pulses will approach a scaling law with a linear dependence on N. Consequently, for high repetition rate pulsing where the cell position won't change much between pulses, the observed effects are expected to scale with N^x, where x is a value exceeding 0.5, and might even reach values larger than one, in case of nonlinear membrane effects. First indications for this were obtained when the time between pulses was reduced from 1 s to 10 ms. The effect on the membrane of B16 cells, measured by using trypan blue, increased slightly with reduced time between pulses [9].

Other effects which would affect random motion of cells are induced dipole moments, e.g., in rod-shaped bacteria, which will try to align the cell-axis in the direction of the electric field. Their relaxation into a random distribution is determined by the viscosity of the medium. In experiments with Escherichia coli, it has been shown that reducing the time between pulses into the microsecond range increased the lethality of the pulses by more than a factor of two [40].

The scaling law, as shown in the example with platelet aggregation (Fig. 6), not only holds for primary effects on the membrane, such as electroporation, but also for secondary effects, and as long as they are intensity-related, not necessarily linearly, to membrane charging, that means they are stimulated through membrane charging effects. With platelet aggregation for example, this connection between effect and cause is as follows: Nanosecond pulses cause release of calcium from the ER through charging of the ER membrane. The increase in intracellular calcium causes an influx of extracellular calcium which serves as an agent for aggregation. Consequently, aggregation has its cause in the charging of the ER membrane.

Appendix A – $N^{1/2}$ Scaling Factor

A.1 Application to Induced Electric Polarization (Two-dimensional disk particles with plane parallel to electric-field vector)

The value of the resulting electric field value can be calculated using the random walk approach. Following Sommerfeld [38], we can consider the random-walk problem in two dimensions, as in Fig. A.1.

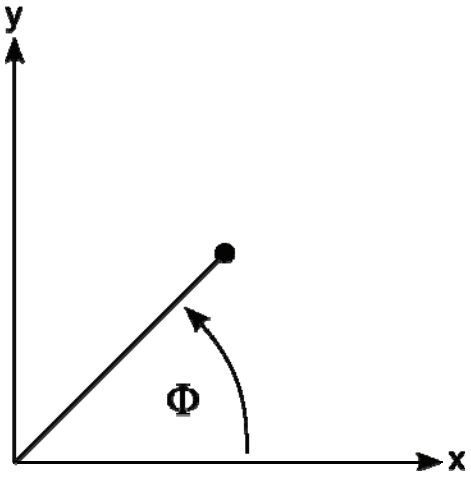

Fig. A.1 Random walk in two dimensions

Starting from the origin we can use complex notation and specify the movement of a particle at step n as

$$e^{j\phi_n} = \cos(\phi_n) + j\sin(\phi_n) \tag{A1}$$

with the real part giving the x motion and the imaginary part giving the y motion. The position of the particle after N steps (each of the same length, but random ϕ_n) is

$$l_N = \sum_{n=1}^{N} e^{j\phi_n} \tag{A2}$$

with each ϕ_n distributed uniformly over 2π radians. The step length is here taken as 1, but this scales to any length.

Then we have

$$\left|l_N\right|^2 = l_N l_N^* = \left[\sum_{n=1}^{N} e^{j\phi_n}\right]\left[\sum_{n=1}^{N} e^{-j\phi_n}\right] = \left[\sum_{n=1}^{N} l_n\right]\left[\sum_{n=1}^{N} l_n^*\right] \tag{A3}$$

$avg\left|l_n\right|^2 \equiv \overline{l_N}^2$ (overbar meaning average, rms sense)

$$= \frac{1}{(2\pi)^N} \int_0^{2\pi} \int_0^{2\pi} \ldots \int_0^{2\pi} |l_N|^2 \, d\phi_N \ldots d\phi_1$$

$$= \frac{1}{(2\pi)^N} \int_0^{2\pi} \int_0^{2\pi} \ldots \int_0^{2\pi} \left[l_1 l_1^* + l_1 \sum_{m=2}^{N} l_m^* + l_1^* \sum_{m=2}^{N} l_m + \left[\sum_{m=2}^{N} l_m \right] \left[\sum_{m=2}^{N} l_m^* \right] \right] d\phi_1 \ldots d\phi_N$$

$$= 1 + \frac{1}{(2\pi)^N} \int_0^{2\pi} \int_0^{2\pi} \ldots \int_0^{2\pi} \left[l_1 \sum_{m=2}^{N} l_m^* + l_1^* \sum_{m=2}^{N} l_m + \left[\sum_{m=2}^{N} l_m \right] \left[\sum_{m=2}^{N} l_m^* \right] \right] d\phi_1 \ldots d\phi_N$$

Integrating terms like

$$l_1 \sum_{m=2}^{N} l_m \tag{A4}$$

over ϕ_1 is zero due to uniform distribution at l_1 in ϕ_1. Integrating

$$\left[\sum_{m=2}^{N} l_m^* \right] \left[\sum_{m=2}^{N} l_m \right] \tag{A5}$$

over ϕ_1, these being independent of ϕ_1, gives 2π. So we have

$$\overline{l_N}^2 = 1 + \frac{1}{(2\pi)^{N-1}} \int_0^{2\pi} \ldots \int_0^{2\pi} \left[\sum_{m=2}^{N} l_m \right] \left[\sum_{m=2}^{N} l_m^* \right] d\phi_2 \ldots d\phi_N \tag{A6}$$

This is exactly like the first form except there are N-1 integrals over terms with the sum starting at 2. By induction then

$$\overline{l_N}^2 = 1 + 1 + \ldots + 1 \text{ (N terms)} = N \tag{A7}$$

and

$$\overline{l_N} = N^{1/2} \tag{A8}$$

The application of N randomly distributed vectors of the same amplitude (in this calculation we used unit vectors) is equivalent to the application of one vector with an amplitude of the square root of N times the amplitude of the single vector. This means for the case of multiple applied pulses of equal field amplitude to biological cells (which change their position with respect to the electric field direction randomly) the effect on the cell membrane can be described as due to a single electric field pulse, with an amplitude of $N^{1/2}$ times that of the applied field amplitude:

$$E = N^{1/2} E_0 \tag{A9}.$$

This result was derived for disk-shaped cells (two-dimensional approach), but also holds for disk-shaped cells, such as platelets and for rod-shaped cells, such as certain bacteria, in a slightly modified form, as will be shown. The $N^{1/2}$ dependence is well known for statistical effects in physics. Such an effect was first reported by Robert Brown in 1826, the so-called Brownian motion of colloidal particles. Replacing E in (16) with this expression provides us scaling law, identical to the empirical expression (4) for nanosecond pulse effects on biological cells.

$$S=S(E_0\tau N^{1/2}) \tag{A10}$$

Applied to electric polarization a pulse of electric field, say in the ϕ_1 direction, induced a polarization p_1 in the ϕ_1 direction. The particle rotates to ϕ_2 and the same additional polarization p_2, now in the ϕ_2 direction, etc. This gives the same result, i.e.,

$$\overline{p} = p_0 N^{1/2} \tag{A11}$$

where p_0 is the magnitude of the polarization induced by a single pulse.

The above assumes that the second pulse comes sufficiently later in time, such that its orientation is uniformly randomly distributed when the second pulse arrives.

This derivation is based on two dimensions for the particle orientation and an electric field that is parallel to this plane. What about other dimensionalities (one to three) for the electric-field and particle orientation?

A.2. Three-dimensional particles taken as spheres in electric-field pulses

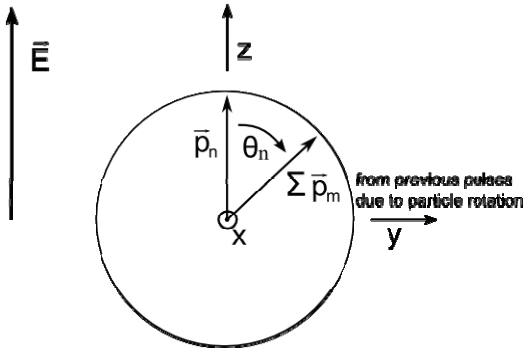

Fig. A.2 Spherical particle

Here θ_n is the spherical polar angle between the old net polarization vector (N-1 step) and the new added $\vec{p}_n$ with

$$\left|\vec{p}_n\right| = p_0 \text{ (all additions of same magnitude)} \tag{A12}$$

Now we have

$$\left|\vec{p}_n\right|^2 = \vec{p}_N \cdot \vec{p}_N \tag{A13}$$

$$= \left[\vec{p}_N + \sum_{n=1}^{N-1} \vec{p}_n\right] \cdot \left[\vec{p}_N \cdot \sum_{n=1}^{N-1} \vec{p}_n\right]$$

with average value given by repeated integrals of the form

$$\frac{1}{4\pi} \int_0^{2\pi} \int_0^{\pi} (...) \sin(\theta) \cos(\theta) d\theta d\phi \tag{A14}$$

Let

$$\overline{P}_N^2 = N \text{-fold average over } 4\pi \text{ steradians over } \theta_n \text{ and } \phi_n \tag{A15}$$

Relate step N to step N-1

$$\overline{P}_N^2 = \frac{1}{(4\pi)^N} \int_0^{2\pi} \int_0^{\pi} ... \int_0^{2\pi} \int_0^{\pi} \left[\vec{p}_N + \sum_{n=1}^{N-1} \vec{p}_n\right] \cdot \left[\vec{p}_N + \sum_{n=1}^{N-1} \vec{p}_n\right] \sin(\theta_1) d\theta_1 d\phi_1 ... \sin(\theta_N) d\theta_N d\phi_N$$

(N double integrals) (A16)

$$= p_0^2 + \frac{1}{(4\pi)^N} \int_0^{2\pi} \int_0^{\pi} ... \int_0^{2\pi} \int_0^{\pi} \left[2 \cdot \vec{p}_N \cdot \sum_{n=2}^{N-1} \vec{p}_n + \left|\sum_{n=1}^{N-1} \vec{p}_n\right|^2\right] \sin(\theta_1) d\theta_1 d\phi_1 ... \sin(\theta_N) d\theta_N d\phi_N$$

The integrals over $2 \cdot \vec{p}_N \cdot \left[\sum_{n=2}^{N-1} \vec{p}_n \sin(\theta_n) d\theta_n d\phi_n\right]$ vanish for a $n \neq 1$ since the $\vec{p}_n$ are uniformly distributed, each over 4π steradians. This leaves

$$\overline{P}_N^2 = p_0^2 + \frac{1}{(4\pi)^N} \int_0^{2\pi} \int_0^{\pi} ... \int_0^{2\pi} \int_0^{\pi} \left|\sum_{n=2}^{N-1} \vec{p}_n\right|^2 \sin(\theta_1) d\theta_1 d\phi_1 ... \sin(\theta_N) d\theta_N d\phi_N \tag{A17}$$

The integrand, no longer being a function of θ_1, except for the $\sin(\theta_1)$ term, reduces by an integral over θ_1 and ϕ_1, to an N-1 fold double integral as

$$\overline{P}_N^2 = p_0^2 + \frac{1}{(4\pi)^N} \int_0^{2\pi} \int_0^{\pi} ... \int_0^{2\pi} \int_0^{\pi} \left|\sum_{n=2}^{N-1} \vec{p}_n\right|^2 \sin(\theta_2) d\theta_2 d\phi_2 ... \sin(\theta_N) d\theta_N d\phi_N \tag{A18}$$

This N-1-fold double integral looks just like the original N-fold double integral. For convenience now rotate the coordinate system so that $\vec{p}_{N-1}$ lines up with the z axis, say the z_{N-1} axis (similarly redefining x_{N-1} and y_{N-1}). This gives

$$\overline{P}_N^2 = \left|\vec{p}_N\right|^2 + \left|\vec{p}_{N-1}\right|^2 + \ldots \text{ (N-2 fold integral)} \tag{A19}$$

By induction this gives

$$\overline{P}_N^2 = \sum_{n=1}^{N}\left|\vec{p}_n\right|^2 = \sum_{n=1}^{N}\left|\vec{p}_0\right|^2 = N\cdot\left|\vec{p}_0^{\,2}\right| = N\cdot\vec{p}_0^{\,2} \tag{A20}$$

$$\overline{P}_N = p_0 N^{1/2}$$

A.3 Needle in three dimensions

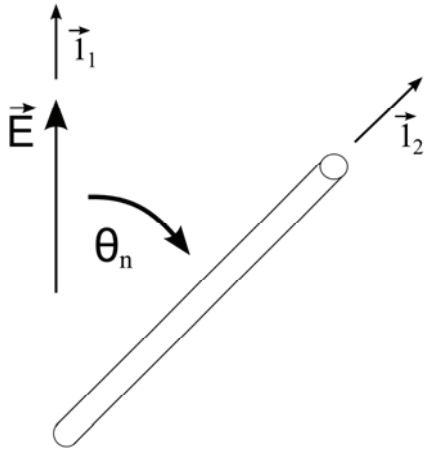

Figure A.3 Rod-like particle

p_0 = induced electric dipole moment if $\vec{l}_1 = \vec{l}_2$ (A21)

$$\vec{p}_1 = \vec{l}_2\cdot\vec{l}_1\vec{l}_1\,p_0 = \cos(\theta_1)\vec{l}_1\,p_0$$

$$\vec{p}_2 = \vec{l}_2\cdot\vec{l}_2\vec{l}_2\,p_0 = \cos(\theta_2)\vec{l}_2\,p_0$$

Sum and average over 4π steradians with $\vec{l}_n$ uniformly distributed

$$\vec{P}_N = \sum_{n=1}^{N}\vec{p}_n \tag{A22}$$

$$\left|\vec{P}_N\right|^2 = \left[\sum_{n=1}^{N}\vec{p}_n\right]\cdot\left[\sum_{n=1}^{N}\vec{p}_n\right]$$

Again, we average by repeated integrals of the form

$$\frac{1}{4\pi}\int_0^{2\pi}\int_0^{\pi}(...)\sin(\theta)d\theta d\phi \tag{A23}$$

So we have, pulling out the $\vec{P}_N\cdot\vec{P}_N$ term

$$\overline{P}_N^2 \equiv avg\vec{P}_N\cdot\vec{P}_N = \frac{1}{(4\pi)^N}\int_0^{2\pi}\int_0^{\pi}...\int_0^{2\pi}\int_0^{\pi}\left[\sum_{n=1}^{N}\vec{p}_n\right]\cdot\left[\sum_{n=1}^{N}\vec{p}_n\right]\sin(\theta_1)d\theta_1 d\phi_1...\sin(\theta_N)d\theta_N d\phi_N$$

$$= p_0^2\frac{1}{4\pi}\int_0^{2\pi}\int_0^{\pi}\cos^2(\theta_N)\sin(\theta_N)d\theta_N d\phi_N + \frac{1}{(4\pi)^N}\int_0^{2\pi}\int_0^{\pi}...\int_0^{2\pi}\int_0^{\pi}\left[2\vec{p}_N\cdot\sum_{n=1}^{N-1}\vec{p}_n + \left|\sum_{n=1}^{N-1}\vec{p}_n\right|^2\right]\sin(\theta_1)d\theta_1 d\phi_1...\sin(\theta_N)d\theta_N d\phi_N \tag{A24}$$

The integrals over $2\vec{p}_N\cdot\sum_{n=2}^{N}\vec{p}_n$ all vanish as before. We also have

$$1_N = \frac{1}{4\pi}\int_0^{2\pi}\int_0^{\pi}\cos^2(\theta_N)\sin(\theta_N)d\theta_N d\phi_N = \frac{1}{2}\int_0^{\pi}\cos^2(\theta_N)\sin(\theta_N)d\theta_N$$

$$= \int_0^{\pi/2}\cos^2(\theta_N)\sin(\theta_N)d\theta_N \tag{A25}$$

Let $\nu = \cos(\theta_N),\ d\nu = -\sin(\theta_N)d\theta_N$

$$1_1 = \int_0^1 \nu^2 d\nu = \frac{1}{3} \tag{A26}$$

This gives

$$\overline{P}_N^2 = \frac{1}{3}p_0^2 + \frac{1}{(4\pi)^{N-1}}\int_0^{2\pi}\int_0^{\pi}...\int_0^{2\pi}\int_0^{\pi}\left[\sum_{n=1}^{N-1}\vec{p}_n\right]\cdot\left[\sum_{n=1}^{N-1}\vec{p}_n\right]\sin(\theta_N)d\theta_N d\phi_N \tag{A27}$$

which is now an N-1 fold double integral. Proceeding as before we find

$$\overline{P}_N^2 = \frac{1}{3}\left[p_0^2 + ...(\text{N terms})\right] = \frac{N}{3}p_0^2 \tag{A28}$$

$$\overline{P}_N = \left[\frac{N}{3}\right]^{1/2} p_0$$

A.4 Circular disk in three dimensions

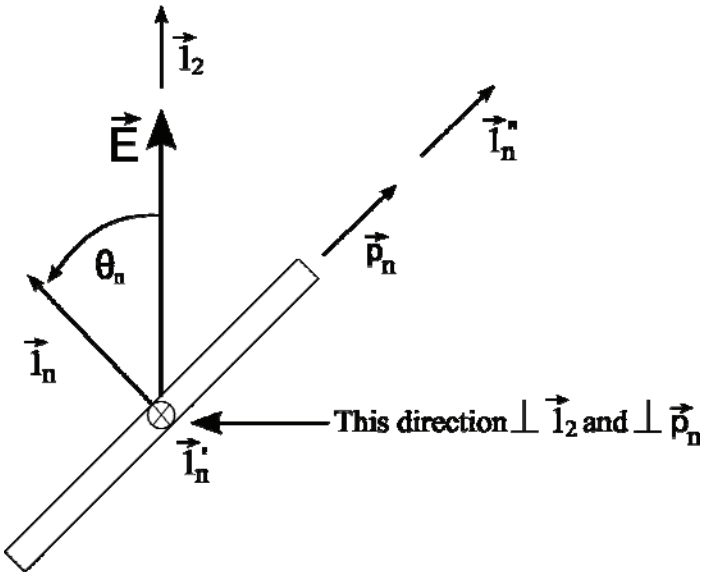

Figure A.4 Disk-like particle

Now take our unit vector $\vec{l}_n$ as perpendicular to the plane of the disk. This makes

$$\vec{p}_n = p_0 \sin(\theta_n)\vec{l}_n'' \tag{A29}$$

$$\vec{p}_n \cdot \vec{p}_n = p_0^2 \sin^2(\theta_n)$$

Proceeding as in Section 3, now we need to integrate

$$\vec{p}_N \cdot \vec{p}_N = p_0^2 \sin^2(\theta_N) \tag{A30}$$

as

$$p_0^2 \frac{1}{4\pi} \int_0^{2\pi} \int_0^{\pi} \sin^3(\theta_N) d\theta_N d\phi_N$$

$$= p_0^2 \frac{1}{2} \int_0^{\pi} \sin^3(\theta_N) d\theta_N$$

$$= p_0^2 \frac{1}{2} \int_0^{\pi} \left[\sin(\theta_N) - \cos^2(\theta_N)\sin(\theta_N)\right] d\theta_N$$

We have these two integrals before, giving

$$p_0^2 \int_0^{\frac{\pi}{2}} \left[\sin(\theta_N) - \cos^2(\theta_N)\sin(\theta_N)\right] d\theta_N \qquad \text{(A31)}$$

$$= p_0^2 \left[1 - \frac{1}{3}\right] = \frac{2}{3} p_0^2$$

By the previous inductive procedure

$$\overline{P}_N = \left[\frac{2N}{3}\right]^{1/2} p_0 \qquad \text{(A32)}$$

A.5 General form of results for 3-dimensional random cell rotation

We find that the above results take the form

$$P_N = [gN]^{1/2} P_O \qquad \text{(A33)}$$

So, in every case, P_N is proportional to $N^{1/2}P_O$, but with a geometric coefficient where

g = 1 for spherical geometry (A34)
g = 2/3 for circular-disk geometry
g = 1/3 for rod geometry

In each case, P_O represents the induced polarization for a single-pulse electric field oriented in a direction to give maximum polarization. The surface electric field (and field across the cell membrane) is proportional to this polarization by additional factors dependent on the geometry and cell constitutive parameters.

References

1. Staempfli, R. 1958. Reversible Breakdown of the Excitable Membrane of a Ranvier Node. An. Acad. Brasil. Ciens. Brazil. 30:57-59.
2. Neumann, E., and K. Rosenheck. 1972. Permeability Changes Induced by Electrical Impulses in Vesicular Membranes, J. Membrane Biol. 10:279-290.
3. Schoenbach, K.H., S.J. Beebe, and E.S. Buescher, 2001. Intracellular Effect of Ultrashort Electrical Pulses. J. Bioelectromagnetics. 22:440-448.
4. Esser, A. T., T. R. Gowrishankar, K. C. Smith, Z. Vasilkoski and J. C. Weaver. 2008. Cell and organelle electropermeabilization and molecular transport through dynamic nanopores. Submitted.
5. Buescher, E. S., and K. H. Schoenbach, 2003. Effects of submicrosecond, high intensity pulsed electric fields on living cells-intracellular electromanipulation. IEEE Trans. Dielectr. and Elect Insul. 10:788-794.
6. Vernier, P.T., Y.H. Sun, L. Marcu, C. M. Craft,, and M. A. Gundersen. 2004. Nanosecond pulsed electric fields perturb membrane phospholipids in T lymphoblasts. FEBS Lett. 572:103-108.

7. White, J. A., P. F. Blackmore, K. H. Schoenbach, and S. J. Beebe. 2004. Stimulation of capacitative calcium entry in HL-60 cells by nanosecond pulsed electric fields. J. Biol. Chem. 279:22964-22972.
8. Buescher, E. S., R. R. Smith, and K. H. Schoenbach. 2004. Submicrosecond intense pulsed electric field effects on intracellular free calcium: Mechanisms and effects. IEEE Trans. Plasma Sci. 32:1563-1572.
9. Zhang, J., P.F. Blackmore, B.Y. Hargrave, S. Xiao, S.J. Beebe, and K.H. Schoenbach. 2008. The Characteristics of Nanosecond Pulsed Electrical Field Stimulation on Platelet Aggregation in Vitro. Arch. Biochem. Biophys. 471:240-248.
10. Beebe, S. J., P. M. Fox, L. J. Rec, E. L. Willis, and K. H. Schoenbach. 2003. Nanosecond, high-intensity pulsed electric fields induce apoptosis in human cells. FASEB J. 17:1493-1495.
11. Beebe, S. J., P. F. Blackmore, J. White, R. P. Joshi, and K. H. Schoenbach. 2004. Nanosecond pulsed electric fields modulate cell function through intracellular signal transduction mechanisms. Physiol. Meas. 25:1077-1093.
12. Beebe, S. J., J. White, P. F. Blackmore, Y. Deng, K. Somers, and K. H. Schoenbach. 2003. Diverse effects of nanosecond pulsed electric fields on cells and tissues. DNA Cell Biol. 22:785-796.
13. Vernier, P.T., A. Lei, L. Marcu, C. M. Craft, and M. A. Gundersen. 2003. Ultrashort Pulsed Electric Fields Induce Membrane Phopholipid Translocation: Differential Sensitivities of Jurkat T Lymphoblasts and Rat Glioma C6 Cells. IEEE Trans. Dielectr. and Electr. Insul. 10:795-809.
14. Nuccitelli; R., U. Pliquett, X. Chen, W. Ford, J. Swanson, S. J. Beebe, J. F. Kolb, and K. H. Schoenbach, 2006. Nanosecond pulsed electric fields cause melanomas to self-destruct. BBRC. 343:351-360.
15. Tieleman, D., H. Leontiadou, A.E. Mark, and S.J. Marrink, 2003. Simulation of Pore Formation in Lipid Bilayers by Mechanical Stress and Electric Fields. J. Am. Chem. Soc. 125:6382-6383.
16. Hu, Q., S. Viswanadham, R. P. Joshi, K. H. Schoenbach, S. J. Beebe, and P. F. Blackmore. 2005 Simulations of transient membrane behavior in cells subjected to a high-intensity ultrashort electric pulse. Phys. Rev. E. 71:031914/1-9.
17. Hu, Q., S. Viswanadham, R. P. Joshi, J. Kolb, and K. H. Schoenbach. 2006. Molecular Dynamics Analysis of High Electric Pulse Effects on Bilayer Membranes Containing DPPC and DPPS. IEEE Trans. Plasma Sci. 34:1405-1411.
18. Hu, Q., R. P. Joshi, and K. H. Schoenbach. 2005. Simulations of Nanopore Formation and Phosphatidylserine Externalization in Lipid Membranes Subjected to a High-Intensity, Ultra-Short Electric Pulse. Phys. Rev. E. 72:031902/1-10.
19. Vernier, P.T., M.J. Ziegler, Y. Sun, M.A. Gundersen, and D.P. Tieleman. 2006. Nanopore-facilitated, voltage-driven phosphatidylserine translocation in lipid bilayers - in cells and in silico. Phys. Biol. 3:233-247.
20. Joshi, R.P., Q. Hu, R. Aly, K.H. Schoenbach, and H.P. Hjalmarson. 2001. Self-consistent simulations of electroporation dynamics in biological cells subjected to ultrafast electrical pulses. Phys. Rev. E. 64:11913/01–3.
21. Joshi, R.P., Q. Hu, K.H. Schoenbach, and H.P. Hjalmarson. 2002. Improved energy model for membrane electroporation in biological cells subjected to electrical pulses. Phys. Rev. E. 65:041920/01-07.

22. Smith, K.C., T.R. Gowrishankar, A.T. Esser, D.A. Stewart, and J.C. Weaver. 2006. The Spatially Distributed Dynamic Transmembrane Voltage of Cells and Organelles due to 10 ns Pulses: Meshed Transport Networks. IEEE Trans. Plasma Science. 34:1394-1404.
23. Kotnik, T. and D. Miklavcic. 2006. Theoretical Evaluation of Voltage Inducement on Internal Membranes of Biological Cells Exposed to Electric Fields. Biophys. J. 90:480-491.
24. Beebe, S. J., P. F. Blackmore, J. White, R. P. Joshi, and K. H. Schoenbach. 2004. Nanosecond Pulsed Electric Fields Modulate Cell Function Through Intracellular Signal Transduction Mechanisms. Physiol. Meas. 25:1077-1093.
25. Pakhomov, A.G., A. Phinney, J. Ashmore, K. Walker III, J.F, Kolb, S. Kono, K.H. Schoenbach, and M.R. Murphy. 2004. Characterization of the Cytotoxic Effect of High-Intensity, 10-ns Duration Electrical Pulses. IEEE Trans. Plasma Sci. 32:1579-1586.
26. Pakhomov, A.G., K. Walker, J.F. Kolb, K.H. Schoenbach, B. Stuck, and M.R. Murphy, (2004) The rules of cell survival after exposure to high-intensity, ultrashort electrical pulses. 2004 Bioelectromagnetics Society.
27. Hall, E. J. 1994. Radiobiology for the Radiologist, 4th ed. Lippincott, Philadelphia.
28. Nias, A. H. W. 1998. An Introduction to Radiobiology, 2nd ed. Wiley, Chichester.
29. Sun, Y., S. Xiao, J. A. White, J. F. Kolb, M. Stacey, and K H. Schoenbach. 2007. Compact, Nanosecond, High Repetition-Rate, Pulse Generator for Bioelectric Studies. IEEE Trans. Diel. Electr. Insul. 14:863-870.
30. Schoenbach, K. H., S. Xiao, R. P. Joshi, J. T. Camp, T. Heeren, J. F. Kolb, and S. J. Beebe. 2008. The Effect of Intense Subnanosecond Electrical Pulses on Biological Cells. IEEE Trans. Plasma Sci. 36:414-422.
31. Neumann, E., 1989. The relaxation hysteresis of membrane electroporation. In Electroporation and Electrofusion in Cell Biology. E. Neumann, A.E. Sowers, and C.A. Jordan, editors, Plenum/New York. 61–82.
32. Melikov, K. C., V. A. Frolov, A. Shcherbakov, A. V. Samsonov, Y. A. Chizmadzhev, and L. V. Chernomordik. 2001. Voltage-Induced Nonconductive Pre-Pores and Metastable Single Pores in Unmodified Planar Lipid Bilayer. Biophys. J. 80:1829-1836.
33. Vasilkoski, Z., A. T. Esser, T. R. Gowrishankar and J. C. Weaver. 2006. Membrane electroporation: The absolute rate equation and nanosecond timescale pore creation. Phys. Rev. E. 74:021904/01-12.
34. Frey, W., J.A. White, R.O. Price, P.F. Blackmore, R.P. Joshi, R. Nuccitelli, S.J. Beebe, K.H. Schoenbach, and J.F. Kolb. 2006. Plasma Membrane Voltage Changes During Nanosecond Pulsed Electric Field Exposure. Biophys. J. 90:3608-3615.
35. Schoenbach, K.H., R.P. Joshi, J.F. Kolb, N. Chen, M. Stacey, P.F. Blackmore, E. S. Buescher, and S.J. Beebe. 2004. Ultrashort Electrical Pulses Open a New Gateway into Biological Cells. Proc. IEEE. 92:1122-1137.
36. Cole, K.S., 1937. Electric Impedance of Marine Egg Membranes. Trans. Faraday Soc., 33:966-972.
37. Reilly, J. P. 1998. Applied Bioelectricity, Springer, New York. chapter 6.3.
38. Sommerfeld, A., 1959. Optik, paragraph 33. In Vorlesungen ueber Theoretische Physik, Vol. IV, Akademische Verlagsgesellschaft, Leipzig.
39. Ibey, B. L., S. Xiao, K. H. Schoenbach, M. R. Murphy, and A. G. Pakhomov. 2008. Plasma membrane permeabilization by 60- and 600-ns electric pulses is determined by the absorbed dose. Submitted to J. Bioelectromagnetics.

40. Aly, R. E., R. P. Joshi, R. H. Stark, K. H. Schoenbach, and S.J. Beebe, (2001) The Effect of Multiple, Microsecond Electrical Pulses on Bacteria. 2001 Pulsed Power and Plasma Science Conference.